Emulsion stabilizing properties of citrus pectin and its interactions with conventional emulsifiers in oil-in-water emulsions

Verkempinck, S.H.E.[1*], Kyomugasho, C.[1], Salvia-Trujillo, L.[1/2], Denis, S.[1], Bourgeois, M.[1], Van Loey, A.M.[1], Hendrickx, M.E.[1], Grauwet, T.[1]**

[1] Laboratory of Food Technology and Leuven Food Science and Nutrition Research Centre (LFoRCe), Department of Microbial and Molecular Systems (M^2S), KU Leuven, Kasteelpark Arenberg 22, PB 2457, 3001, Leuven, Belgium

[2] Food Technology Department, University of Lleida, Rovira Roure 191, 25198 Lleida, Spain

Author's email addresses:

Verkempinck, S.H.E.: sarah.verkempinck@kuleuven.be

Kyomugasho, C.: clare.kyomugasho@kuleuven.be

Salvia-Trujillo, L.: lsalvia@tecal.udl.cat

Denis, S.: denis.sofie@gmail.com

Bourgeois, M.: marjan_bourgeois@hotmail.com

Van Loey, A.M.: ann.vanloey@kuleuven.be

Hendrickx, M.E.: marceg.hendrickx@kuleuven.be

Grauwet, T.: tara.grauwet@kuleuven.be

Journal: Food Hydrocolloids

Submitted: March 2018

Resubmitted: May 2018

Resubmitted II: July 2018

*author whom correspondence should be addressed during submission process:

sarah.verkempinck@kuleuven.be

+32 16 37 63 32

** author whom correspondence should be addressed post-publication:

tara.grauwet@kuleuven.be

+32 16 32 19 47

Graphical abstract:

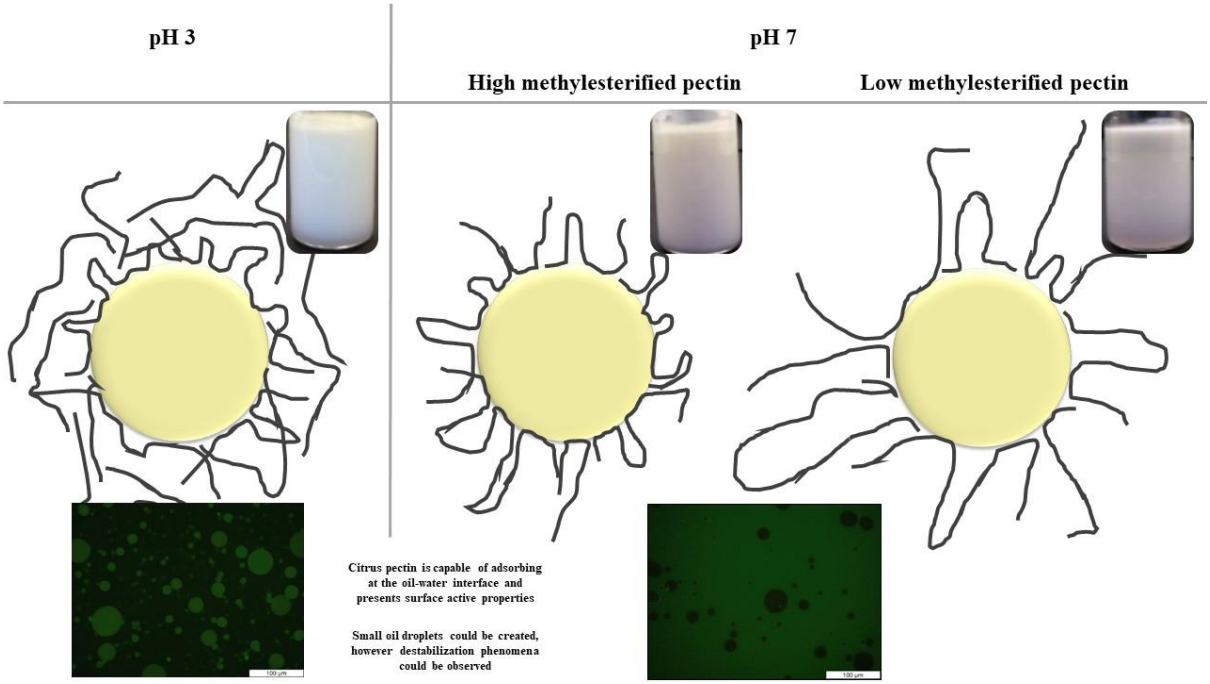

Highlights:

- Citrus pectin is a surface-active molecule
- Addition of citrus pectin allows creation of emulsions with small droplet sizes
- Pectin structure influences its organization at the oil droplet surface
- Emulsion acidity determines the way pectin stabilizes the oil droplet interface
- Combination of pectin and conventional emulsifier led to depletion flocculation

Abstract

The present work focused on the *(i)* physical characterization of the emulsion stabilizing potential of citrus pectin (CP) with different degree of methylesterification (DM; CP82, CP38 and CP10) and *(ii)* evaluation of interactions that occur between CP and conventional emulsifiers (Tween80 and phosphatidylcholine) used for emulsion stabilization.

Firstly, the emulsifying properties of different samples were studied by evaluating the electrical charge, hydrodynamic radius, adsorbed layer thickness and change in interfacial tension. The results showed that the pectin charge was strongly dependent on its DM and pH of the aqueous phase. For example, the hydrodynamic volume and adsorbed layer thickness of CP10 were larger compared to CP38 and CP82 at neutral pH due to the presence of more chargeable carboxylic groups. Moreover, it was quantitatively shown that CP is capable of reducing the interfacial tension of an oil droplet regardless its DM, evidencing its adsorption at the oil-water interfaces and surface active properties.

Secondly, the physicochemical stability of oil-in-water emulsions was evaluated during short-term storage at 4°C. All pectin-emulsions showed the formation of a cream layer after one day. However, the nature and extent of this layer depended on the emulsion composition. All pectin single-emulsifier stabilized emulsions presented a cream layer most likely caused by bridging flocculation induced by the pectin structures. Contrastingly, depletion flocculation was observed in case of the multiple-emulsifier stabilized emulsions. In all cases, the destabilization phenomena observed were reversible as the particle size did not dramatically change over storage time, showing that CP has emulsion stabilizing potential.

Keywords: citrus pectin, emulsion, stability, degree of methylesterification

Abbreviations:

CP: citrus pectin

CP82; CP38 or CP10: citrus pectin with a degree of methylesterification of 82%, 38% and 10%, respectively

CP82 emulsion: 5% (w/v) olive oil-in-water emulsion stabilized with 1% (w/v) citrus pectin with a degree of methylesterification of 82%

CP38 emulsion: 5% (w/v) olive oil-in-water emulsion stabilized with 1% (w/v) citrus pectin with a degree of methylesterification of 38%

CP10 emulsion: 5% (w/v) olive oil-in-water emulsion stabilized with 1% (w/v) citrus pectin with a degree of methylesterification of 10%

DB_{abs}: absolute degree of blockiness

DM: degree of methylesterification

GalA: galacturonic acid

HMP: high methylesterified pectin

LMP: low methylesterified pectin

MF: Melamine fluoride

MMP: medium methylesterified pectin

o/w emulsion: oil-in-water emulsion

PC: Phosphatidylcholine

PC emulsion: 5% (w/v) olive oil-in-water emulsion stabilized with 1% (w/v) phosphatidylcholine

PCCP82 emulsion: 5% (w/v) olive oil-in-water emulsion stabilized with 1% (w/v) phosphatidylcholine and 1% (w/v) citrus pectin with a degree of methylesterification of 82%

PCCP38 emulsion: 5% (w/v) olive oil-in-water emulsion stabilized with 1% (w/v) phosphatidylcholine and 1% (w/v) citrus pectin with a degree of methylesterification of 38%

PCCP10 emulsion: 5% (w/v) olive oil-in-water emulsion stabilized with 1% (w/v) phosphatidylcholine and 1% (w/v) citrus pectin with a degree of methylesterification of 10%

PME: pectin methylesterase

PS: polystyrene

TW: Tween 80

TW emulsion: 5% (w/v) olive oil-in-water emulsion stabilized with 0.5% (w/v) Tween 80

TWCP82 emulsion: 5% (w/v) olive oil-in-water emulsion stabilized with 0.5% (w/v) Tween 80 and 1% (w/v) citrus pectin with a degree of methylesterification of 82%

TWCP38 emulsion: 5% (w/v) olive oil-in-water emulsion stabilized with 0.5% (w/v) Tween 80 and 1% (w/v) citrus pectin with a degree of methylesterification of 38%

TWCP10 emulsion: 5% (w/v) olive oil-in-water emulsion stabilized with 0.5% (w/v) Tween 80 and 1% (w/v) citrus pectin with a degree of methylesterification of 10%

1 Introduction

Oil-in-water (o/w) emulsions are interesting delivery systems of lipophilic bioactive compounds, such as vitamins and antioxidants (McClements, 2010). These emulsions are thermodynamically unstable systems, consisting of dispersed oil droplets in a continuous, aqueous phase. Emulsifiers are often added to kinetically stabilize o/w emulsions and the type being used depends on the desired product shelf life, stability and functionality. Most commonly used emulsifier types in food industry are small molecule surfactants, biopolymers and phospholipids (McClements, 2016a). Besides, there is an increasing interest for more natural ingredients from both costumer and industry sides (McClements & Gumus, 2016; Alba & Kontogiorgos, 2017). Several proteins, polysaccharides and phospholipids belong to this category of emulsifiers which can be extracted from natural resources. In the past, extensive research was already performed to investigate the emulsifying properties of different proteins (e.g. whey protein, β-lactoglobulin and caseinates) to stabilize o/w emulsions (Dickinson, 1994; Elizalde, Bartholomai, & Pilosof, 1996; DEMETRIADES, COUPLAND, & McClements, 1997; Tokle & McClements, 2011; Qian et al., 2012). By contrast, only limited information is available regarding the emulsion stabilizing properties of certain polysaccharides and phospholipids. In this context, pectin represents an interesting polysaccharide, naturally present in plants.

Pectin is a group of polysaccharides rich in galacturonic acid (GalA) units and predominantly located in the primary cell wall and middle lamella of higher plants (Willats et al., 2001). Pectin can be extracted from several plant sources, but commercially available pectin sources are mainly citrus peel, apple pomace and sugar beet pulp (Chan et al., 2017). The variation in pectin structure and composition results in different functionalities of which its gel-forming capacity was extensively studied in the past (Lofgren et al., 2005; Fraeye et al., 2010; Ngouémazong et al., 2012). Recently, more attention is given to the emulsifying and

emulsion-stabilizing properties of pectin. These emulsifying and emulsion-stabilizing properties are determined by both intrinsic (e.g. degree of methylesterification, protein content, acetyl groups and molecular weight) as well as extrinsic (e.g. pectin concentration, pH and ionic strength) factors (Ngouémazong et al., 2015; Alba & Kontogiorgos, 2017). Pectin is a biopolymer used for its emulsion stabilization properties, because the addition of the polymer can lead to an increased viscosity of the aqueous phase of an o/w emulsion (Dickinson, 2003). In addition, it may confer negative charge (pH > ~3.5) in the surrounding areas of oil droplets due to its anionic nature, contributing to the electrostatic stability of o/w emulsions (Morris, Foster, & Harding, 2000). However, it has been recently suggested that pectin might actually act as a surface active emulsifier. In this context, although being a water-soluble polymer, pectin might have some slightly hydrophobic moieties (e.g. acetyl groups and methylesters) that provide pectin the ability to adsorb at the oil-water interface (Schmidt et al., 2015b; Chen, Fu, & Luo, 2016; Schmidt, Schütz, & Schuchmann, 2017; Kpodo et al., 2018). For example, commercially available citrus pectin with medium (55%) and high (70% and 84%) degree of methylesterification is able to create stable emulsions at low pH (pH 2-4) (Schmidt et al., 2017). Nevertheless, the exact mechanism and the actual adsorption capacity remains unrevealed as well as the possible interactions between pectin and conventional emulsifiers in o/w emulsions.

Therefore, the first part of this work focuses on exploring the emulsifying properties of citrus pectin with distinct degree of methylesterification at low and neutral pH. More specifically, several physical characteristics of the different pectin samples are evaluated: pectin charge, hydrodynamic diameter and adsorbed layer thickness. In addition, a dynamic interfacial tension evaluation was performed and is measured for both pure pectin solutions as well as for pectin in presence of a conventional emulsifier, namely Tween 80. This dynamic evaluation allows the determination of both the adsorption rate as well as the final emulsion

surface tension value. In the second part, the emulsifying properties are evaluated during a short-term storage study using the different citrus pectin samples as single-emulsifier or in a multiple-emulsifier solution in which citrus pectin will be combined with a more conventional emulsifier, such as Tween 80 or phosphatidylcholine. It was hypothesized that possible interactions could occur in case of the multiple-emulsifier emulsions and therefore could influence the organization and stability of the emulsion. The overall results of this work lead to a proposed hypothesis on how pectin is organized in the different emulsions (pectin only, pectin combined with Tween 80 or pectin combined with phosphatidylcholine) at two distinct pH values, which was visualized by fluorescently labeling the pectin and corresponding microscopic images.

2 Material and methods

2.1 Materials

High methylesterified citrus pectin (HMP) was obtained from Sigma Aldrich (Diegem, Belgium) and used to prepare medium and low methylesterified citrus pectin (MMP and LMP, respectively). Orange carrots (*Daucus carota* cv. Nerac), kiwis (*Actinidia deliciosa* cv. Hayward) and olive oil were bought in a local shop. The carrots were peeled, cut into small pieces, frozen with liquid nitrogen and stored at -40 °C until extraction of pectin methylesterase (PME). The PME inhibitor was extracted from ripened kiwis. Melamine fluoride (MF) and polystyrene (PS) microspheres were purchased from microParticles GmbH (Berlin, Germany) and had an average diameter of 1.04 µm (± 0.03) and 1.05 µm (± 0.03), respectively. All analytical chemicals and reagents were purchased from Sigma Aldrich (Diegem, Belgium), VWR Chemicals (Leuven, Belgium) or Acros Organics (Geel, Belgium). Ultrapure water (organic free, 18.2 MΩ cm resistance) was used for all sample preparations and was supplied by a Simplicity™ 150 water purification system (Millipore, Billerica, USA).

2.2 Pectin preparation

MMP and LMP were obtained through enzymatic demethylesterification of HMP as described by Ngouémazong et al. (2011). Carrot pectin methylesterase (PME) removes methyl esters blockwise, creating long contiguous stretches of demethylesterified carboxylic groups (Jolie et al., 2010) which might be of interest for its emulsifying properties.

First, the enzyme PME was extracted from carrots and purified according to the procedure described by Jolie et al. (2009). Briefly, carrot puree was mixed with Tris-HCl buffer (pH 8) containing 0.1 M NaCl (1:1.3 w/v) overnight at 4 °C to extract the PME from the carrots. The PME-extract was purified through affinity chromatography with PME inhibitor from kiwi and concentrated using different centrifugation steps (Vivaspin 20 with Molecular weight

cut-off = 5 x 10^3 g/mol, Sartorius, Germany; JA-14 rotor, Beckman Coulter, USA). An automatic titration (718 STAT titrino, Metrohm, Switzerland) was used to determine PME activity and the concentrated PME-extract was stored at -80 °C until further use. Secondly, pectin was demethylesterified by dissolving 0.8% CP82 in 0.1 M sodium phosphate buffer (pH 7) and incubating this pectin solution with PME at 30 °C for different time periods. PME was inactivated by reducing the pH of the pectin solution to pH 4.5 and applying a heat shock (4 min, 85 °C) (Ngouémazong et al., 2011). Hereafter, the pectin solutions were immediately cooled (4 °C) and the pH was adjusted to pH 6 so the carboxylic groups are negatively charged which is important for determining the DM (section 2.3). Finally, the pectin solutions were dialyzed for 48 hours (Spectra/Por®, Molecular weight cut-off = 12-14 x 10^3 g/mol) against demineralized water at 4 °C and lyophilized (Christ Alpha 2-4 LSC, Germany).

2.3 Pectin structure characterization

The pectin samples obtained were characterized in terms of DM, absolute degree of blockiness (DB_{abs}), molecular weight and protein content. The pectin DM was determined using Fourier transform infra-red (FT-IR) spectroscopy (IRAffinity-1, Shimadzu, Japan) following the method and calibration curve described by Kyomugasho et al. (2015). Since the mother pectin was enzymatically modified, a blockwise organization of the carboxylic groups is expected. Therefore, the DB_{abs} was estimated using the polynomial function determined by Ngouémazong et al. (2011), which quantitatively represents the distribution pattern of methylesters in each pectin sample. The procedure of Shpigelman et al. (2014) was used to evaluate the molecular weight distributions of the different pectin samples. High performance size exclusion chromatography (HPSEC) was used to elute pectin structures based on their hydrodynamic volume. Pectin samples (2% w/v) were dissolved in ultrapure water and incubated at 65 °C for 15 minutes to facilitate subsequent filtration. Subsequently, these pectin solutions were filtered (Chromafil PET filter, 0.45 µm pore size, 25 mm diameter) and

injected (100 µL). The HPLC system was equipped with a series of three columns (Ultrahydrogel 250, 1000 and 2000; Waters, Milford, USA) kept at 35 °C and different detectors, namely a multi-angle laser light scattering (MALS) detector (PN3621, Postnova analytics, Germany), a refractive index (RI) detector (Shodex RI-101, Showa Denko K.K., Kawasaki, Japan), a diode array detector (DAD) (Agilent Technologies, Diegem, Belgium) and a viscometer (PN3310, Postnova analytics, Landsberg am Lech, Germany). A flow rate of 0.5 mL/min of 0.1 M acetic acid buffer with 0.1 M $NaNO_3$ was applied. The molecular weight of all samples was obtained using the software provided by the MALS detector manufacturer (NovaMALS 1.2.0.0, Postnova analytics, Germany) (Shpigelman et al., 2014) and the dn/dc value was taken as 0.146 mL/g (Shpigelman et al., 2014). Lastly, the Dumas method was used to determine the protein content of all pectin samples, since proteins have emulsifying properties. An automatic elemental analyzer (Carlo-Erba EA1108, Thermo Scientific, Waltham, MA, USA) was used to measure the nitrogen content of each pectin sample. A conversion factor of 6.25 was applied to calculate the protein content. The analysis was performed in duplicate.

2.4 Exploring the emulsifying properties of citrus pectin

The different pectin samples were investigated at the level of their emulsifying properties. For that reason, the effect of the pectin concentration and pH was evaluated on the pectin electrical charge (section 2.4.1). Additionally, the hydrodynamic diameter and adsorbed layer thickness of the different pectin samples were measured as an attempt to study the colloidal size of the biopolymer in aqueous solution and the capacity to adsorb to different particle surfaces, respectively (sections 2.4.2 and 2.4.3, respectively). Lastly, the dynamic interfacial tension was measured to evaluate the surface active properties of the emulsifiers studied (section 2.4.4).

2.4.1 ζ-potential

The emulsifying potential of pectin was explored firstly through the determination of pectins ζ-potential at different concentrations using an automated capillary electrophoresis equipment (Zetasizer NanoZS, Malvern Instruments, Worcestershire, UK). Different pectin concentrations (0.25-3% w/v) were prepared in ultrapure water and the pH was afterwards adjusted to pH 3 or 7 with HCl or NaOH, respectively. Pectin solutions were further diluted 1:100 (v/v) with ultrapure water set at pH 3 or 7 and transferred into a capillary cell having two electrodes. An electrical voltage was applied over the electrodes, resulting in particle movement which was influenced by the particle charge. The velocity of the hydrocolloid was monitored and used to determine the electrophoretic mobility. Finally, the equation of Henry was applied by the instrument's software to determine the ζ-potential of the measured particles. A similar measurement was performed with 1% (w/v) pectin solutions in a broad pH range (2-7) to evaluate the charge of the different pectin structures in the pH range of plant-based food systems. All ζ-potential measurements were performed in duplicate.

2.4.2 Hydrodynamic diameter

The hydrodynamic diameter of the different pectin samples was measured to evaluate the size of the pectin with different DM in solution and the impact of pH on this size, according to the procedure described by Schmidt, Schütz & Schuchmann (2017). Briefly, solutions with different pectin concentrations (0.01-0.25% v/v) were prepared at pH 3 as well as pH 7. These pectin solutions were further diluted 1:1 with ultrapure water (pH 3 or 7, respectively) and transferred into a macro UV-cuvette. Each concentration was measured twice in terms of size using the dynamic light scattering principle of the zetasizer instrument (Zetasizer NanoZS, Malvern Instruments, Worcestershire, UK). Laser light was diffracted and energy was transferred, which accelerates the particle movement depending on their size. Analysis of this Browning motion using the Stokes-Einstein relationship resulted in a particle size. Each

pectin concentration was measured twice with a minimum of 12 runs. The detected particle size was plotted against the corresponding pectin concentration and extrapolated to zero to obtain the hydrodynamic diameter of each pectin sample at a certain pH (Schmidt et al., 2017).

2.4.3 Adsorbed layer thickness

The adsorbed layer thickness of all pectin samples to both PS as well as MF microspheres was measured in order to investigate the possible pectin organization at a droplet surface. Both the PS particles as well as the pectin samples are negatively charged at low pH, giving an indication about the hydrophobic interactions occurring with pectin. Oppositely, the MF microspheres are positively charged at low pH, which could give more information about the electrostatic interactions with pectin. Briefly, a 2% (w/v) pectin solution (pH 3 or 7) was mixed 1:1 overnight with 0.5% (v/v) microspheres (pH 3 or 7) as described by Schmidt et al. (2017). The particle size in this mixture was measured in triplicate using the zetasizer instrument, as described above. As the size of the PS and MF microspheres was known (section 2.1), the adsorbed pectin layer thickness could be calculated from the difference in size measured for adsorbed and non-adsorbed MF or PS microspheres.

2.4.4 Dynamic interfacial tension

Finally, a pendant drop tensiometer (CAM 200, KSV Instruments, Finland) was used as described by Dopierala et al. (2011) to evaluate the change in interfacial tension caused by the different pectin samples in comparison with a conventional emulsifier, namely Tween 80 (TW). Pectin single-solutions (1% w/v, pH 3 or 7) were prepared and used for the measurement as such or as multiple-emulsifier solutions in combination with 0.5% (w/v) TW. In this way, the emulsifying potential of the individual and combined emulsifier structures can be explored as an indication of possible competitive adsorption. Purified olive oil was used to form a droplet at the tip of a U-shaped needle, while the emulsifier solutions were

located in a cuvette. The olive oil was purified to remove all surface-active molecules by following the procedure of Bahtz et al. (2009), with some minor modifications. Briefly, 10 g Florisil was rotated for 2 hours with 50 mL of olive oil, whereafter the oil was filtered and stored in dark until use. It was opted to use purified olive oil for the experiments to study the effect of the emulsifier(s) only on the change in interfacial tension. The pendant drop measurements recording the changes in the interfacial tension were performed for 2 hours and in duplicate.

2.5 Emulsion preparation

O/w emulsions were prepared by mixing 5% (w/v) olive oil and an emulsifier solution for 10 minutes at 9500 rpm (Ultra-Turrax T25, IKA, Staufen, Germany), resulting in a coarse emulsion. The emulsifier concentration in solution depended on the emulsifier type, namely 0.5% (w/v) TW, 1% (w/v) citrus pectin (CP), 1% (w/v) phosphatidylcholine (PC) or a combination of these emulsifiers (TWCP or PCCP) was used to stabilize the emulsions. The coarse emulsion was further stabilised by applying a high pressure homogenisation step at 100 MPa (Pressure Cell Homogenizer, Stansted Fluid Power LTD., UK). The pH of all emulsions was adjusted to pH 3 or pH 7 using HCl or NaOH. The emulsions were stored at 4 °C, protected from light and oxygen. An emulsion stabilised with 0.5% Tween 80 and 1% citrus pectin with a DM of 82 will be indicated as 'TWCP82'. Overall, 11 different emulsion types were prepared and studied at both pH 3 and 7, in analogy being referred to as TW; CP82; CP38; CP10; TWCP82; TWCP38; TWCP10; PC; PCCP82; PCCP38 and PCCP10. The emulsions stabilized by one emulsifier type (i.e. TW; PC and CP) will be called 'single-emulsifier stabilized emulsions', while the emulsions stabilized by citrus pectin in combination with Tween 80 or phosphatidylcholine (i.e. TWCP and PCCP) will be referred to as 'multiple-emulsifier stabilized emulsions'.

2.6 Physicochemical stability of emulsions

The physicochemical stability of all emulsions was evaluated by performing a storage experiment. All emulsions were stored at 4 °C for 4 days. The particle electrical charge, particle size and creaming index of all emulsions was determined, and visually monitored by taking photographic images.

2.6.1 Particle electrical charge

The oil droplets ζ-potential was measured based on the principle of electrophoretic mobility and dynamic light scattering using an automated capillary electrophoresis equipment (Zetasizer NanoZS, Malvern Instruments, Worcestershire, UK). Samples were prepared and measured as described before (section 2.4). The ζ-potential obtained describes the charge of the measured oil droplet.

2.6.2 Particle size

A laser diffraction equipment (Beckman Coulter Inc., LS 13 320, Miami, Florida, USA) was used to determine the particle size of the emulsions. Emulsions were shaken, brought into a stirring tank filled with demineralized water and pumped (speed 30%) to the measurement cells. There, particles diffract the laser light (wavelength main illumination source: 750 nm; wavelengths halogen light for Polarization Intensity Differential Scattering (PIDS): 450 nm; 600 nm; 900 nm) whereafter the intensity is detected, analyzed with the Fraunhofer model and transformed to particle sizes. The reported d_{43} value is the mean volume-weighted particle size. Volume-weighted particle sizes were preferred as these are more prone to the presence of a small amount of large particles and so is a more sensitive indicator for emulsions instability than surface-weighted particle sizes.

2.6.3 Creaming index

The creaming index of the emulsions was measured daily. Capped, glass tubes were filled with 5 mL of emulsion and the total height was measured using a caliper (Mitutoyo Belgium, Kruibeke, Belgium). The height of the upper cream layer was measured daily, allowing to calculate the creaming index. The creaming index (%) is expressed as the ratio of the height of the upper, cream layer (mm) to the height of the total emulsion (mm). Tubes used for determination of the creaming index were not shaken during this storage experiment.

2.7 Visualization of the microstructure of citrus pectin-based coarse emulsions

The microstructure of the pectin containing emulsions were visualized using fluorescent microscopy as described by Nordmark & Ziegler (2000) with the aim of visually strengthening the proposed stabilizing mechanisms of the emulsions under consideration. More specifically, each pectin sample was labeled with the non-ionic fluorescent dye BODIPY FL hydrazide (4,4-difluoro-5,7-dimethyl-4-bora-3a,4adiaza-s-indacene-3-propionylhydrazide). As described in section 2.5, coarse emulsions were prepared by mixing 5% (w/v) olive oil with an emulsifier solution (10 minutes at 9500 rpm), containing 1% (w/v) CP, a combination of 0.5% TW and 1% CP or a combination of 1% PC and 1% CP. The acidity of these coarse emulsions was adjusted to pH 3 or 7. Hereafter, the microstructure of each coarse emulsion was visualized using the Olympus BX-41 microscope (Olympus, Optical Co. Ltd., Tokyo, Japan) equipped with epifluorescence illumination (X-Cite Fluorescence Illumination, Series 120Q EXFO Europe, Hants, United Kingdom) and Image-analysis software (cell*, Soft Imaging System, Münster, Germany). It was opted to visualize the microstructure of the coarse emulsion since oil droplets of this particle size can be better visualized in comparison to oil droplets with smaller particle sizes as a consequence of high pressure homogenization of the coarse emulsion. All images were taken with the same settings.

2.8 Statistical analysis

All statistical analyzes were performed using the statistical software JMP (JMP Pro13, SAS Institute Inc., Cary, NC, USA). Significant differences in hydrodynamic diameter and pectin adsorption thickness were determined calculating the 95% confidence intervals. One way ANOVA and Tukey's Studentized Range Post-hoc test with a 95% level of significance ($p<0.05$) was used to evaluate significant differences in particle charge and size of all samples.

3 Results and discussion

3.1 Emulsifying properties of citrus pectin with different degree of methylesterification

In a first part, the emulsifying potential of citrus pectin with different DM was evaluated based on different structural and physical characteristics. The results obtained are described in detail in the following sections.

3.1.1 Structural properties of citrus pectin

All results regarding the structural properties of the citrus pectin samples are summarized in **Table 1**. The average DM of each pectin sample was measured. The values obtained for HMP, MMP and LMP were 82.2% (± 1.2), 38.3% (± 0.9) and 10.4% (± 1.0), respectively. Therefore, these pectin samples will be further referred to as CP82, CP38 and CP10. It must be noted that these values are averages, representing the DM of the main population of the pectin samples. In addition, the DB_{abs} was calculated and the resulting values were 10.8% (± 0.9); 51.0% (± 1.0) and 85.9% (± 1.3) for CP82, CP38 and CP10, respectively. As expected (Celus et al., 2018), enzymatically decreasing the DM resulted in an increased DB_{abs}. The molecular weight was determined as this could influence the emulsifying properties of pectin (Akhtar et al., 2002; Leroux et al., 2003). The resulting weight-average molecular weights were 58.7 ± 1.3 x 10^3 g/mol, 54.5 ± 2.0 x 10^3 g/mol and 54.1 ± 1.2 x 10^3 g/mol for CP82, CP38 and CP10, respectively. These results show that the use of PME for the reduction of pectin DM did not significantly change the molecular weight. Additionally, the concentration distribution as function of elution time of the different pectin samples is shown in **Figure 1**. Lastly, the protein content of the pectin samples was evaluated since these functional units can improve the emulsifying potential of pectin by acting as hydrophobic anchors at the interface (Alba & Kontogiorgos, 2017). The protein content was 1.72% (± 0.01), 1.44%

(± 0.01) and 1.55% (± 0.03) for CP82, CP38 and CP10, respectively. These values are comparable to the ones of apple pectin (~1.6%) (Kravtchenko, Voragen, & Pilnik, 1992), but rather low compared to the protein content of sugar beet pectin (~5%) (Chen et al., 2016), tomato serum pectin (~11%) or broccoli serum pectin (up to ~33%) (Santiago et al., 2018). Therefore, it is assumed that the protein content will only have a minor influence on the emulsifying properties of the pectin samples studied. To conclude, the results of the structural characterization of the different pectin samples allows to attribute possible differences in emulsifying potential of citrus pectin to its degree of methylesterification only.

3.1.2 Pectin electrical charge as function of concentration and pH

Pectin polymers are built up from galacturonic acid units which can be methylesterified at the C-6 carboxyl group (Mohnen, 2008). These carboxylic groups can be negatively charged depending on the pH of the continuous phase and will influence the functional properties of the pectin structure (Sila et al., 2009). Therefore, the ζ-potential of the different pectin samples (CP82, CP38 and CP10) was measured in terms of pectin concentration and pH of the aqueous phase (**Figure 2A and B**, respectively).

In general, negative charges were observed, showing that the CP samples are anionic as was expected. The effect of pectin concentration on the charge of pectin was limited. From a 0.75-1% (w/v) pectin concentration onwards, the charge did not significantly change. Therefore, a 1% (w/v) pectin concentration was chosen to conduct the following experiments. Moreover, previous research showed that oil-in-water (o/w) emulsions with small initial oil droplet sizes could be produced with a pectin concentration of 1% (Verrijssen et al., 2014; Schmidt et al., 2015a). From **Figure 2B** it can be seen that pectin solutions at low pH (pH 2) barely carried any charge (-8 to 0 mV). The increase of pH allowed proton release from the free carboxyl groups present in the pectin structure, resulting in a higher charge density of the pectin chains. For example, the ζ-potential of a 1% CP95 solution changed from -7.6 mV to -34.1

mV when the acidity of the solution was altered from pH 3 to pH 7. Moreover, the DM had a significant impact on the ζ-potential change, as more demethylesterified pectin can carry more negative charges. For instance, the ζ-potential dropped from -7.6 mV to -20.1 mV and -21.0 mV, when the pectin DM decreased from 82% to respectively, 38% and 10% at pH 3. Similar observations apply to and were even more distinct in case of the pectin solutions at pH 7. Upon reaching the pKa value (around 3.38 to 4.10), 50% of the free carboxyl groups are negatively charged and an inflection point in the curve was observed (**Figure 2B**). Lastly, it could be noted that even below the pKa, pectin structures carry a negative charge, which was more pronounced for pectin with lower DM. Two pH levels were selected to be further studied, namely pH 3 and 7 as these conditions are relevant for the acidity of fruit- and vegetable-based products as well as the acidity of the gastric and small intestinal phase. The latter can be of interest for future work, since the emulsion stability along the digestive tract can determine the (lipid) digestion extent (Verkempinck et al., 2018).

3.1.3 Hydrodynamic diameter of citrus pectin samples

The hydrodynamic diameter D_h of the different pectin samples is presented in **Table 2**. In general, a higher D_h was observed for the samples having a higher particle charge. At pH 3, no significant differences were observed between CP82 and CP38 (227-230 nm), while their D_h is significantly smaller than the one of CP10 (270 nm). All pectin samples carried almost no charges at pH 3 (**Figure 2B**) since this pH was below the pKa value of the pectin structures (section 3.1.2). Nevertheless, a small fraction of carboxyl groups of CP10 was ionized, probably leading to some intramolecular repulsion and an increased D_h compared to CP82 and CP38. By contrast, at pH 7, all three pectin samples had a significantly different D_h, which was increasing with a decreasing pectin DM. At pH 7, all pectin samples are above their pKa value, resulting in a large fraction of negatively charged carboxyl groups (section 3.1.2). The presence of these negative charges caused inter- and intramolecular repulsion,

leading to an increased D_h of all pectin samples compared to the D_h at pH 3. Moreover, the lower the DM, the more negatively charged carboxylic groups were present in the pectin structure (CP10 > CP38 > CP82). Therefore, it can be postulated that the intramolecular repulsion was most pronounced for CP10, resulting an increased volume occupation and thus D_h. The results obtained were of the same magnitude as those reported by Schmidt et al. (2017). For example, citrus pectin with a DM of 84% at pH 3 had a D_h of around 280 nm in their study. Additionally, and similar to our results, these researchers showed that the differences in D_h between citrus pectin samples with different DM is more pronounced with increasing pH.

3.1.4 Adsorbed layer thickness of pectin

In order to evaluate the possible organization of pectin at an oil-water interface, the pectin adsorbed layer thickness was determined of the different pectin samples, using polystyrene (PS) and melamine fluoride (MF) microspheres with a known diameter (1.04 ± 0.03 µm and 1.05 ± 0.03 µm, respectively). The PS microspheres were negatively charged, while the MF microspheres were positively charged. The results obtained are shown in **Table 3**. Determination of the 95% confidence intervals showed no significant differences in the pectin layer thickness adsorbed for the different pectin samples at pH 3 with both microsphere types. In case of the PS microspheres, the adsorbed layer had a size of 989-1064 nm which is around 4 times the hydrodynamic volume of pectin (section 3.1.3). The adsorbed layer at the MF particles was somewhat smaller and had a size of 826-886 nm. These observations led to the hypothesis that the almost neutral pectin samples (section 3.1.2) can adsorb at the particle in multilayers. Similar observations were made with okra and sugar beet pectin (Alba, Sagis & Kontogiorgos (2016) and Siew et al. (2008), respectively), and were partially attributed to the lower hydrodynamic diameter of pectin at low pH, allowing pectin to adsorb at the interface in a multilayered way. This type of steric organization was

visualized by Alba & Kontogiorgos (2017). In **Figure 3**, a schematic representation of our hypothetical organization of pectin at the oil-water interface is shown. The small difference in adsorbed layer thickness at the PS and MF particles could be attributed to the different functional groups determining the charge of the microspheres. Methylol and imino groups bring a positive charge to the MF particles, while sulfate groups produce a negative charge for the PS particles. It can be hypothesized that the negatively charged pectin samples can form a more compact multilayer when adsorbing to an opposite charged surface, namely the positively charged MF particles.

The layer thickness of the adsorbed pectin structures was of different sizes at pH 7 (**Table 3**). At high pH, the pectin conformation is more extended as almost all carboxyl groups are ionized (i.e. section 3.1.2). Consequently, more inter- and intramolecular repulsion occurs which can lead to fewer groups adsorbing at the oil-water interface (Alba & Kontogiorgos, 2017). It can be postulated that at high pH, pectin is adsorbing to droplets in a loop-tail way and stabilizes the droplet in an electrostatic way. Hereby, the hydrophobic regions (such as acetyl and methyl groups) attach at the oil-water interface, while the hydrophilic regions (charged galacturonic acid components) stay in the continuous phase. Especially in case of CP38 and CP10, its structures can support this hypothesis since these pectin samples have a blockwise organization of carboxylic groups created by the enzymatic demethylesterification treatment by plantPME. The loop-tail organization of pectin was visualized by Leroux et al. (2003) and more recently by Alba & Kontogiorgos (2017). In **Figure 3**, we depict our hypothetical drawing of the organization of HMP and LMP at the oil-water interface in a neutral environment. The adsorbed pectin layer thickness of the pectin samples at pH 7 were of different magnitude in comparison to pH 3. This could be attributed to the negative charges of CP which increased with a lower pectin DM. The lower the pectin DM is, the more negative charges will be present at pH 7 (**Figure 2B**) and the less flexible the pectin

494 structure will be (Morris et al., 2000). Hence, it can be assumed that the lower the pectin DM
495 is, the more extended the organization will be at the droplet interface leading to a larger
496 adsorbed layer thickness and more exposed interface.

497 **3.1.5 Evaluation of the oil droplet interfacial tension**

498 **Figure 4** shows the results obtained of the dynamic interfacial tension of an olive oil droplet
499 present in a single-emulsifier solution (0.5% TW or 1% CP with different DM) or multiple-
500 emulsifier solution (0.5% TW mixed with 1% CP with different DM) at pH 3 and 7. As a
501 reference, the interfacial tension of the purified olive oil was measured against ultrapure
502 water at pH 3 or 7. It could be observed that, for this reference, the interfacial tension only
503 slightly changes, showing that the olive oil was relatively free of surface-active components,
504 such as polyphenols.

505 In general, it could be observed that all emulsifier solutions were able to decrease the
506 interfacial tension of the olive oil droplet (**Figure 4**). In addition, no effect of pH of the
507 emulsifier solutions was detected.

508 Of all single-emulsifier solutions, the TW solution was the fastest in decreasing the oil
509 droplet interfacial tension and the final interfacial tension reached, was the lowest of all
510 conditions studied. The former could be attributed to the lower molecular weight of TW
511 (≈1200-1350 Da) in comparison with the CP samples (≈ 60 x 10^3 g/mol; section 2.3).
512 Therefore, it can be postulated that TW can adsorb much faster to the oil-water interface and
513 subsequently decreases the interfacial tension. Among the CP samples, an effect of pectin
514 DM on the change in interfacial tension could be observed. The CP82 single-emulsifier
515 decreased the interfacial tension of the oil droplet to a lower plateau value than the CP38 and
516 CP10 single-emulsifiers both at pH 3 as well as pH 7. HMP can be assumed to have a more
517 hydrophobic character compared to MMP and LMP as a limited number of chargeable
518 carboxyl groups are present. Consequently, it has long stretches which are methylesterified

519 causing CP82 to occupy the oil-water interface in a higher extent in comparison to CP38 and
520 CP10.

521 In case of the multiple-emulsifier TWCP solutions, the rate with which the interfacial tension
522 of the oil droplet is decreased is similar or even slightly faster than of the single-emulsifier
523 TW solution. Consequently, it can be hypothesized that the TW emulsifier with low
524 molecular weight adsorbed at the oil-water interface, while the CP structures remained in
525 solution. In addition, the presence of both TW as well as CP in the multiple-emulsifier
526 solution probably provided an additional driving force for TW to adsorb at the oil droplet,
527 resulting in a faster decrease of the interfacial tension and lower final plateau values in
528 comparison with the single-emulsifier TW. In these cases, no effect of pectin DM could be
529 observed, which could be attributed to the assumption that CP did not adsorb at the oil-water
530 interface, but remained in the surrounding medium.

531 **3.2 Physicochemical stability of emulsions with pectin addition**

532 Based on the results obtained in the first part of this study (section 3.1), it could be
533 hypothesized that CP has emulsifying potential at both low as well as neutral pH. Therefore,
534 o/w emulsions were created and stabilized with 0.5% TW, 1% PC, 1% CP with different DM
535 or a combination of CP with TW or PC (i.e. TWCP and PCCP multiple-emulsifier stabilized
536 emulsions, respectively). The pH of these emulsions was adjusted to pH 3 or 7, whereafter
537 they were stored at 4 °C for 4 days. The physicochemical stability of all emulsions was
538 evaluated by determination of the particle charge, particle size and creaming index, in
539 combination with visual observations. The results obtained will be discussed in the following
540 sections. It must be noted that non-purified olive oil was used, containing surface-active
541 components such as polyphenols, which can attribute to emulsion stability by, for example,
542 decreasing the interfacial tension (Dopierala et al., 2011). However, the use of non-purified
543 olive oil was opted for since this comes more close to a realistic food system.

3.2.1 Electrical charge

The electrical charge of emulsified oil droplets was measured to evaluate the emulsifiers behavior at the interface and the interactions between the emulsified oil droplets and components present in the surrounding medium (e.g. pectin). **Figure 5** shows the results of the ζ-potential of all emulsions in function of storage time at 4 °C. In general, it could be observed that the ζ-potential did not dramatically change during the short storage experiment. The emulsions stabilized with the non-ionic TW was negatively charged at both pH 3 as well as pH 7, which might be attributed to the presence of impurities in the oil phase (i.e. free fatty acids; FFA) or the preferential adsorption of hydroxyl ions from the continuous phase to the hydrophilic head of the surfactants (McClements, 2016b). Oppositely, the emulsions stabilized with the zwitterionic (i.e. carrying both positive as well as negative charges) phosphatidylcholine (PC) presented a slightly positive charge at pH 3 which could be explained by the shielding of the negatively charged phosphate groups by hydrogen ions at low pH (Lin et al., 2014). The emulsions stabilized with pectin only presented a negative charge, influenced by both the DM of the pectin structures and the pH of the aqueous phase. The results showed that the pectin emulsions had a charge between -10 and -30 mV at pH 3 (**Figure 5A**), whereby the emulsion charge became more negative with a decreased pectin DM as more chargeable non-methylesterified groups were present. At this low pH, the pectin samples were below their pKa value, but still some carboxylic groups were negatively charged as was described in section 3.1.2. At pH 7, the pectin emulsions presented even more negative charges as almost all carboxylic groups were negatively charged. The ζ-potential of the emulsions stabilized with both TW and CP, had a similar particle charge as the TW emulsion (at both pH values studied) (**Figure 5B**). TW is a non-ionic surfactant with hydrophilic-lipophilic balance value 15 and a relatively low molecular weight, while all pectin samples had a much higher molecular weight of around 60 x 10^3 g/mol (section 2.3). It

569 can be hypothesized that the small TW molecules adsorbed much faster at the oil-water
570 interface during the homogenization step(s) than the large pectin structures. Hence, TW
571 probably covered the complete oil droplet surface in case of these TWCP emulsions, while
572 pectin remained in the aqueous phase. Consequently, the TWCP emulsions could exhibit the
573 same charge pattern as the TW emulsion. This hypothesis is supported by the results
574 discussed in section 3.1.5, showing that the TWCP combination reduced the interfacial
575 tension as fast as in the emulsion where TW was solely present. By contrast, the PCCP
576 multiple-emulsifier stabilized emulsions did not show the same charge pattern as the PC
577 single-emulsifier stabilized emulsion, but an effect of pectin DM was observed. In the case of
578 the PCCP emulsions, most likely both PC and pectin were located at the oil-water interface to
579 a certain extent despite the low molecular weight of PC (≈ 758-810 Da). PC is known to have
580 an intermediate hydrophobicity (hydrophilic-lipophilic balance value of 2-8) and are often
581 used in combination with other emulsifiers to form stable o/w emulsions (McClements &
582 Gumus, 2016; McClements, 2016b).

583 **3.2.2 Creaming index, particle size and visual observations**

584 The physicochemical stability was evaluated by measuring the upper creaming layer formed,
585 the emulsion particle sizes and by visual evaluation (images). The results from these analysis
586 can be evaluated in **Figure 6**, **Figure 7**, **Figure 8** and **Figure 9**.

587 TW emulsions at both pH 3 and 7 remained stable for 4 days as no upper, cream layer was
588 visible. Moreover, the mean particle size was around 1.3 µm and did not change over storage
589 time, as is visualized by the particle size distribution. Similar particle sizes were observed by
590 Salvia-Trujillo et al. (2017). These observations show that TW is efficient in stabilizing o/w
591 emulsions.

592 Different observations were made for the PC emulsions, which were stable at pH 7 for 4
593 days, but unstable at pH 3. The initial oil droplet size of the PC emulsion at pH 3 (1.61 ± 0.10

μm) was significantly higher than the initial oil droplet size of the PC emulsion at pH 7 (1.04 ± 0.01 μm). Moreover, the former emulsion showed a shift to larger particle size over storage time (2.33 ± 0.02 μm, day 4), while the latter emulsion remained stable in terms of particle size (1.02 ± 0.02 μm, day 4). Research of Comas, Wagner & Tomás (2006) had similar findings and attributed this behavior to the swelling of phospholipids after acid addition. Consequently, the emulsifying capacity of the lecithin diminished leading to simultaneous creaming and coalescence phenomena.

In case of the pectin emulsions, formation of a cream layer was observed for all pectin samples at both pH 3 and 7. The cream layer was thicker at pH 7 in comparison with the emulsions at pH 3, except for the CP82 emulsion. The formation of this cream layer could be attributed to the more extended adsorption of pectin at the oil-water interface at high pH. In sections 3.1.3 and 3.1.4, it was described that on the one hand pectin at pH 7 showed a larger hydrodynamic diameter than at pH 3, and on the other hand organized itself differently at the oil droplet water interface at low or neutral pH. More specifically, at pH 7 it was hypothesized that pectin was adsorbing in a loop-tail way and the lower DM is, the more uncovered spaces were present at the oil droplet. In this way, the high pH might have caused the pectin emulsions to be less stable than at low pH. Nevertheless, a cream layer was also observed for the pectin emulsions a low pH and thus are also considered to be unstable. Additionally, the measured particle sizes only slighted increased after 4 days at both pH 3 and 7. Therefore, the observed cream layer could be attributed to and bridging flocculation and limited coalescence. In addition, the particle size distributions presented a small intensity peak at larger particle sizes. All pectin emulsions had a particle size between 1.5 and 2 μm, showing that CP can be used to form small emulsified oil droplets. Similar droplet sizes were obtained for 1% CP emulsions formulated in a previous study of Verrijssen et al. (2015).

618 The multiple-emulsifier stabilized emulsions, i.e. TWCP and PCCP emulsions, showed a
619 dramatic increase in the cream layer thickness after 1 day of storage, followed by a gradual
620 decrease. Analyzing the images presented in **Figure 9**, complete phase separation was
621 observed in these cases, attributed to the phenomena of depletion flocculation. The presence
622 of pectin in the aqueous phase created an osmotic imbalance between the aqueous phase and
623 the spaces around the oil droplets. This caused water migration from the intervening gap
624 between the oil droplets to the continuous phase, whereby oil droplets were driven towards
625 each other (Dickinson, 2003). Eventually these oil droplets moved upwards due to their lower
626 density than water, so an upper, oil droplet layer and a lower, aqueous layer were observed.
627 The depletion flocculation phenomena were also observed by Surh, Decker & McClements
628 (2006), Gharsallaoui et al. (2010) and Qiu, Zhao & McClements (2015), however all studying
629 emulsions stabilized with pectin and a certain protein type. The thickness of the cream layer
630 was more extended for the PCCP emulsions than for the TWCP emulsions. It was
631 hypothesized (section 3.2.1) that in the former, pectin was located to a certain extent at the
632 oil-water interface, while all pectin was in the aqueous phase in the latter. Therefore, it could
633 be postulated that the osmotic driving force in the PCCP emulsions was smaller in
634 comparison to the TWCP emulsions. Consequently, for the PCCP emulsions the water
635 migration went slower, leading to a thicker cream layer after 4 days of storage compared to
636 the TWCP emulsions. Moreover, multiple-emulsifier stabilized emulsions at pH 7, showed an
637 increased cream layer with decreasing pectin DM. This could be attributed to the more
638 extended structure of CP10 and CP38 compared to CP82, as the presence of less compact
639 pectin structures might have slowed down the water migration process. Only the reversible
640 depletion flocculation phenomenon occurred in the case of the TWCP emulsions as the
641 particle sizes and distributions of these emulsions remained stable during the time period
642 studied (**Figure 7C, 7D and 8**). In the case of the PCCP emulsions, besides depletion

643 flocculation, also coalescence was observed as the particle size of the emulsions slightly
644 increased over 4 days of storage (**Figure 7E, 7F and 8**).

645 ## 3.3 Microstructure of pectin-based emulsions

646 In order to verify the hypothetical organization mechanism of pectin in the emulsions studied
647 (**Figure 3**), microscopic images were taken with fluorescently labelled pectin present in
648 coarse emulsions. In addition, control images of the CP82-based emulsions were taken
649 without the dye at the same magnification and light intensity. Representative micrographs are
650 depicted in **Figure 10**.

651 From the control images, it can be observed that autofluorescence is negligible. Therefore,
652 fluorescent dye was added to visualize pectin. The addition of the small dye molecule is
653 anticipated to have negligible influence on the microstructure of the emulsions.

654 In case of the single-emulsifier emulsions containing CP only, a clear difference could be
655 visualized between the coarse emulsions with pH of 3 on the one hand and the coarse
656 emulsions with a pH of 7 on the other hand. At pH 3, it was postulated (section 3.1) that
657 pectin adsorbs at the oil-water interface in multilayers. The presence of pectin at the droplet
658 surface can be confirmed by the fluorescent micrographs, whereby green-colored oil droplets
659 are observed within a black background. This means that all pectin structures are located at
660 the oil-water interface and none of the pectin remains in the surrounding medium. A different
661 organization was observed at pH 7. All pectin samples carry a high negative charge at neutral
662 pH, which induces inter- and intramolecular repulsion. Consequently, it was hypothesized
663 that at neutral pH, the pectin adsorbs at the oil-water surface in a loop-tail way. This
664 hypothesis is strengthened by the fluorescent micrographs since brown oil droplets were
665 visualized in a green continuous phase. In other words, most of the pectin structures are
666 located in the aqueous phase, while a few pectin structures can adsorb at the interface with

667 their hydrophobic groups attached to the oil droplet and their hydrophilic regions are very
668 likely located in the continuous phase. Subsequently, the majority of the pectin fraction is
669 located in the surrounding aqueous phase, as evidenced by the green fluorescence of the
670 background.

671 For the multiple-emulsifier stabilized emulsions, containing both TW as well as CP, it was
672 hypothesized that TW is present at the oil droplet surface and CP in the aqueous phase
673 (section 3.1). Both for pH 3 as well as pH 7, this was confirmed by the microstructures
674 visualized by fluorescent microscopy. These micrographs clearly show oil droplets (brown
675 colored) surrounded by a fluorescent background (green colored aqueous phase), containing
676 pectin.

677 Lastly, in the case of the PCCP emulsions, it was assumed that both emulsifier types were
678 present at the oil-droplet interface for both pH levels studied (section 3.1). From the
679 micrographs, it can be observed that flocculated structures were formed embedding the oil
680 droplets. At pH 3, it is possible that a double emulsion was created, whereby the PC adsorbed
681 first at the oil-water interface, followed by the negatively charged CP. This mechanism was
682 also suggested by Guo et al. (2017). Surprisingly, these flocculated structures were also
683 observed at pH 7, whereby both PC as well as CP are negatively charged. However, these
684 flocs are broken after high pressure homogenization in both cases (micrographs not shown).

685 To conclude, the micrographs of the coarse emulsions containing pectin, confirm the
686 hypotheses suggested in section 3.1. For the single-emulsifier CP emulsions, pectin is located
687 at the oil-water interface in multilayers when the acidity is low. By contrast, pectin is
688 organized in a loop-tail way in a neutral environment whereby the charged pectin stretches
689 are present in the surrounding medium. In case of the TWCP emulsions, the assumption that
690 TW adsorbs at the oil droplet, while pectin was located in the aqueous phase was confirmed
691 by the micrographs. Lastly, in case of the PCCP emulsions, floc-like structures are created by

692 interactions between PC and CP, in which the oil droplets are embedded. For future work, it
693 could be interesting to gain unambiguous information for all emulsions by visualization of
694 the interface and structural organization in the aqueous phase by using for example cryo-
695 scanning electron microscopy.

4 Conclusions

In the work presented in this paper, the emulsifying properties of citrus pectin with different degree of methylesterification (DM) were explored. Moreover, emulsions were prepared in which a commonly used emulsifier (Tween 80 or phosphatidylcholine) was combined with citrus pectin to evaluate the influence of the presence of pectin on the emulsion stability. It was shown that citrus pectin is a surface-active molecule as it was able to lower the interfacial tension of an oil droplet. Moreover, small initial oil droplets were created when pectin only was used to form an emulsion. In addition, citrus pectin stabilized the emulsions by both steric as well as electrostatic interactions, depending on the pectin DM and pH of the continuous phase. Nevertheless, visually a small cream layer was observed in the emulsions stabilized with pectin only. In the case where pectin was combined with Tween 80 or phosphatidylcholine for emulsion stabilization, a totally different behavior was observed. More specifically, a complete phase separation was detected, regardless of the pectin DM and the pH of the aqueous phase. The combination of two emulsifiers caused pectin to be (partially) in the continuous phase, creating an osmotic imbalance which led to the phenomena of depletion flocculation. This can be of relevance for food product design in which emulsions are mixed with pectin-containing ingredients. Nevertheless, the occurrence of irreversible destabilization phenomena (such as coalescence) was limited. In conclusion, this work showed the potential of citrus pectin as natural emulsifier and/or emulsion stabilizer. In this sense, small oil droplets could be created using pectin as an emulsifier and these emulsions remained stable during short-term storage. By contrast, there is still a challenge regarding the multiple-emulsifier stabilized emulsions which showed phase separation. For future work, it could also be interesting to visualize the emulsifier organization at the oil-water interface and in the aqueous phase by, for example, cryo-scanning electron microscopy. In addition, the emulsion behavior in presence of other

components (e.g. ions and proteins) could be studied. Lastly, the emulsion stability during digestion and its interactions with digestive components (e.g. bile, lipase and calcium) can be evaluated in perspective of food product design taking into account nutritional aspects as well.

Acknowledgment

This research was financially supported by the Institute for the Promotion of Innovation through Science and Technology in Flanders (IWT-Vlaanderen). S.H.E. Verkempinck is a Doctoral Researcher funded by IWT-Vlaanderen (Grant No. 141469). L. Salvia-Trujillo is a Postdoctoral Researcher funded by the European Union's Horizon 2020 research and innovation programme under the Marie Sklodowska-Curie grant agreement No. 654924. In addition, the authors acknowledge the financial support of the KU Leuven Research Council (METH/14/03) through the long termstructural funding–Methusalem funding by the Flemish Government. The authors would like to thank the Division of Soft Matter, Rheology and Technology (KU Leuven, Leuven) for the use of the pendant drop tensiometer.

Declaration of interests

The authors of the present work declare no conflict of interests.

References

Akhtar, M., Dickinson, E., Mazoyer, J., & Langendorff, V. (2002). Emulsion stabilizing properties of depolymerized pectin. *Food Hydrocolloids, 16,* 249-256.

Alba, K. & Kontogiorgos, V. (2017). Pectin at the oil-water interface: Relationship of molecular composition and structure to functionality. *Food Hydrocolloids, 68,* 211-218.

Alba, K., Sagis, L. M. C., & Kontogiorgos, V. (2016). Engineering of acidic O/W emulsions with pectin. *Colloids and Surfaces B: Biointerfaces, 145,* 301-308.

Bahtz, J., Knorr, D., Tedeschi, C., Leser, M. E., Valles-Pamies, B., & Miller, R. (2009). Adsorption of octanoic acid at the water/oil interface. *Colloids and Surfaces B: Biointerfaces, 74,* 492-497.

Celus, M., Salvia-Trujillo, L., Kyomugasho, C., Maes, I., Van Loey, A. M., Grauwet, T. et al. (2018). Structurally modified pectin for targeted lipid antioxidant capacity in linseed/sunflower oil-in-water emulsions. *Food Chemistry, 241,* 86-96.

Chan, S. Y., Choo, W. S., Young, D. J., & Loh, X. J. (2017). Pectin as a rheology modifier: Origin, structure, commercial production and rheology. *Carbohydrate Polymers, 161,* 118-139.

Chen, H. m., Fu, X., & Luo, Z. g. (2016). Effect of molecular structure on emulsifying properties of sugar beet pulp pectin. *Food Hydrocolloids, 54,* 99-106.

Comas, D. I., Wagner, J. R., & Tomás, M. C. (2006). Creaming stability of oil in water (O/W) emulsions: Influence of pH on soybean protein–lecithin interaction. *Food Hydrocolloids, 20,* 990-996.

DEMETRIADES, K., COUPLAND, J. N., & McClements, D. J. (1997). Physical Properties of Whey Protein Stabilized Emulsions as Related to pH and NaCl. *Journal of Food Science, 62,* 342-347.

Dickinson, E. (1994). Protein-stabilized emulsions. *Journal of Food Engineering, 22,* 59-74.

Dickinson, E. (2003). Hydrocolloids at interfaces and the influence on the properties of dispersed systems. *Food Hydrocolloids, 17,* 25-39.

767 Dopierala, K., Javadi, A., Krägel, J., Schano, K. H., Kalogianni, E. P., Leser, M. E. et al.
768 (2011). Dynamic interfacial tensions of dietary oils. *Colloids and Surfaces A:*
769 *Physicochemical and Engineering Aspects, 382,* 261-265.

770 Elizalde, B. E., Bartholomai, G. B., & Pilosof, A. M. R. (1996). The effect of pH on the
771 relationship between hydrophilic/lipophilic characteristics and emulsification
772 properties of soy proteins. *LWT - Food Science and Technology, 29,* 334-339.

773 Fraeye, I., Colle, I., Vandevenne, E., Duvetter, T., Van Buggenhout, S., Moldenaers, P. et al.
774 (2010). Influence of pectin structure on texture of pectin-calcium gels. *Innovative*
775 *Food Science & Emerging Technologies, 11,* 401-409.

776 Gharsallaoui, A., Yamauchi, K., Chambin, O., Cases, E., & Saurel, R. (2010). Effect of high
777 methoxyl pectin on pea protein in aqueous solution and at oil/water interface.
778 *Carbohydrate Polymers, 80,* 817-827.

779 Guo, Q., Ye, A., Bellissimo, N., Singh, H., & Rousseau, D. (2017). Modulating fat digestion
780 through food structure design. *Progress in Lipid Research, 68,* 109-118.

781 Jolie, R. P., Duvetter, T., Van Loey, A. M., & Hendrickx, M. E. (2010). Pectin
782 methylesterase and its proteinaceous inhibitor: a review. *Carbohydrate Research, 345,*
783 2583-2595.

784 Jolie, R. P., Duvetter, T., Houben, K., Clynen, E., Sila, D. N., Van Loey, A. M. et al. (2009).
785 Carrot pectin methylesterase and its inhibitor from kiwi fruit: Study of activity,
786 stability and inhibition. *Innovative Food Science & Emerging Technologies, 10,* 601-
787 609.

788 Kpodo, F. M., Agbenorhevi, J. K., Alba, K., Oduro, I. N., Morris, G. A., & Kontogiorgos, V.
789 (2018). Structure-Function relationships in pectin emulsification. *Food Biophysics,*
790 *13,* 71-79.

791 Kravtchenko, T. P., Voragen, A. G. J., & Pilnik, W. (1992). Analytical comparison of three
792 industrial pectin preparations. *Carbohydrate Polymers, 18,* 17-25.

793 Kyomugasho, C., Christiaens, S., Shpigelman, A., Van Loey, A. M., & Hendrickx, M. E.
794 (2015). FT-IR spectroscopy, a reliable method for routine analysis of the degree of
795 methylesterification of pectin in different fruit- and vegetable-based matrices. *Food*
796 *Chemistry, 176,* 82-90.

797 Leroux, J., Langendorff, V., Schick, G., Vaishnav, V., & Mazoyer, J. (2003). Emulsion
798 stabilizing properties of pectin. *Food Hydrocolloids, 17,* 455-462.

Lin, X., Wang, Q., Li, W., & Wright, A. J. (2014). Emulsification of algal oil with soy lecithin improved DHA bioaccessibility but did not change overall *in vitro* digestibility. *Food & Function, 5,* 2913-2921.

Lofgren, C., Guillotin, S., Evenbratt, H., Schols, H., & Hermansson, A. M. (2005). Effects of calcium, pH, and blockiness on kinetic rheological behavior and microstructure of HM pectin gels. *Biomacromolecules, 6,* 646-652.

McClements, D. J. (2016a). Emulsion Ingredients. In *Food emulsions: Principles, practices, and techniques* (Third edition ed., pp. 99-183). Boca Raton, Florida, USA: CRC Press (Taylor & Francis Group).

McClements, D. J. (2016b). *Food emulsions: Principles, practices and techniques*. (Third ed.) Boca Raton, Florida, USA: CRC Press (Taylor & Francis Group).

McClements, D. J. (2010). Emulsion design to improve the delivery of functional lipophilic components. *Annual Review of Food Science and Technology, 1,* 241-269.

McClements, D. J. & Gumus, C. E. (2016). Natural emulsifiers – Biosurfactants, phospholipids, biopolymers, and colloidal particles: Molecular and physicochemical basis of functional performance. *Advances in Colloid and Interface Science, 234,* 3-26.

Mohnen, D. (2008). Pectin structure and biosynthesis. *Current Opinion in Plant Biology, 11,* 266-277.

Morris, G. A., Foster, T. J., & Harding, S. E. (2000). The effect of the degree of esterification on the hydrodynamic properties of citrus pectin. *Food Hydrocolloids, 14,* 227-235.

Ngouémazong, E. D., Kabuye, G., Fraeye, I., Cardinaels, R., Van Loey, A., Moldenaers, P. et al. (2012). Effect of debranching on the rheological properties of Ca^{2+}-pectin gels. *Food Hydrocolloids, 26,* 44-53.

Ngouémazong, E. D., Tengweh, F. F., Duvetter, T., Fraeye, I., Van Loey, A., Moldenaers, P. et al. (2011). Quantifying structural characteristics of partially de-esterified pectins. *Food Hydrocolloids, 25,* 434-443.

Ngouémazong, E. D., Christiaens, S., Shpigelman, A., Van Loey, A., & Hendrickx, M. (2015). The emulsifying and emulsion-stabilizing properties of pectin: A review. *Comprehensive Reviews in Food Science and Food Safety, 14,* 705-718.

829 Nordmark, T. S. & Ziegler, G. R. (2000). Quantitative assessment of phase composition and
830 morphology of two-phase gelatin-pectin gels using fluorescence microscopy. *Food*
831 *Hydrocolloids, 14,* 579-590.

832 Qian, C., Decker, E. A., Xiao, H., & McClements, D. J. (2012). Physical and chemical
833 stability of β-carotene-enriched nanoemulsions: Influence of pH, ionic strength,
834 temperature, and emulsifier type. *Food Chemistry, 132,* 1221-1229.

835 Qiu, C., Zhao, M., & McClements, D. J. (2015). Improving the stability of wheat protein-
836 stabilized emulsions: Effect of pectin and xanthan gum addition. *Food Hydrocolloids,*
837 *43,* 377-387.

838 Salvia-Trujillo, L., Verkempinck, S. H. E., Sun, L., Van Loey, A. M., Grauwet, T., &
839 Hendrickx, M. E. (2017). Lipid digestion, micelle formation and carotenoid
840 bioaccessibility kinetics: Influence of emulsion droplet size. *Food Chemistry, 229,*
841 653-662.

842 Santiago, J. S., Salvia-Trujillo, L., Palomo, A., Niroula, A., Xu, F., Van Loey, A. M. et al.
843 (2018). Process-induced water-soluble biopolymers from broccoli and tomato purées:
844 Their molecular structure in relation to their emulsion stabilizing capacity. *Food*
845 *Hydrocolloids, 81,* 312-327.

846 Schmidt, U. S., Koch, L., Rentschler, C., Kurz, T., Endreß, H. U., & Schuchmann, H. P.
847 (2015a). Effect of molecular weight reduction, acetylation and esterification on the
848 emulsification properties of citrus pectin. *Food Biophysics, 10,* 217-227.

849 Schmidt, U. S., Schmidt, K., Kurz, T., Endreß, H. U., & Schuchmann, H. P. (2015b). Pectins
850 of different origin and their performance in forming and stabilizing oil-in-water-
851 emulsions. *Food Hydrocolloids, 46,* 59-66.

852 Schmidt, U. S., Schütz, L., & Schuchmann, H. P. (2017). Interfacial and emulsifying
853 properties of citrus pectin: Interaction of pH, ionic strength and degree of
854 esterification. *Food Hydrocolloids, 62,* 288-298.

855 Shpigelman, A., Kyomugasho, C., Christiaens, S., Van Loey, A. M., & Hendrickx, M. E.
856 (2014). Thermal and high pressure high temperature processes result in distinctly
857 different pectin non-enzymatic conversions. *Food Hydrocolloids, 39,* 251-263.

858 Siew, C. K., Williams, P. A., Cui, S. W., & Wang, Q. (2008). Characterization of the surface-
859 active components of sugar beet pectin and the hydrodynamic thickness of the
860 adsorbed pectin layer. *Journal of Agricultural and Food Chemistry, 56,* 8111-8120.

Sila, D. N., Van Buggenhout, S., Duvetter, T., Fraeye, I., De Roeck, A., Van Loey, A. et al. (2009). Pectins in processed fruit and vegetables: Part II - Structure-function relationships. *Comprehensive Reviews in Food Science and Food Safety, 8,* 86-104.

Surh, J., Decker, E. A., & McClements, D. J. (2006). Influence of pH and pectin type on properties and stability of sodium-caseinate stabilized oil-in-water emulsions. *Food Hydrocolloids, 20,* 607-618.

Tokle, T. & McClements, D. J. (2011). Physicochemical properties of lactoferrin stabilized oil-in-water emulsions: Effects of pH, salt and heating. *Food Hydrocolloids, 25,* 976-982.

Verkempinck, S. H. E., Salvia-Trujillo, L., Moens, L. G., Charleer, L., Van Loey, A. M., Hendrickx, M. E. et al. (2018). Emulsion stability during gastrointestinal conditions effects lipid digestion kinetics. *Food Chemistry, 246,* 179-191.

Verrijssen, T. A. J., Balduyck, L. G., Christiaens, S., Van Loey, A. M., Van Buggenhout, S., & Hendrickx, M. E. (2014). The effect of pectin concentration and degree of methyl-esterification on the *in vitro* bioaccessibility of β-carotene-enriched emulsions. *Food Research International, 57,* 71-78.

Verrijssen, T. A. J., Verkempinck, S. H. E., Christiaens, S., Van Loey, A. M., & Hendrickx, M. E. (2015). The effect of pectin on *in vitro* β-carotene bioaccessibility and lipid digestion in low fat emulsions. *Food Hydrocolloids, 49,* 73-81.

Willats, W. G. T., McCartney, L., Mackie, W., & Knox, J. P. (2001). Pectin: cell biology and prospects for functional analysis. *Plant Molecular Biology, 47,* 9-27.

884 **Table 1: Summary of the structural properties of the pectin samples.**

Sample code	DM (%)	DB_{abs} (%)	M_W (x 10^3 g/mol)	Protein content (%)
CP82	82.2 ± 1.2	10.8 ± 0.9	58.7 ± 1.3	1.72 ± 0.01
CP38	38.3 ± 0.9	51.0 ± 1.0	54.5 ± 2.0	1.44 ± 0.01
CP10	10.4 ± 1.0	85.9 ± 1.3	54.1 ± 1.2	1.55 ± 0.03

885

886 **Table 2: Hydrodynamic diameter D_h (nm) of the citrus pectin (CP) samples with different**
887 **degree of methylesterification (DM; 82, 38 or 10%), measured at both pH 3 as well as pH 7.**
888 **Different letters indicate significant differences among the samples (95% confidence interval).**

	Hydrodynamic diameter (nm)
CP82 pH 3	229.8 ± 5.7 [a]
CP38 pH 3	227.0 ± 6.2 [a]
CP10 pH 3	269.8 ± 7.9 [b]
CP82 pH 7	259.8 ± 6.2 [b]
CP38 pH 7	312.5 ± 6.2 [c]
CP10 pH 7	350.2 ± 7.2 [d]

889

890

Table 3: Adsorbed layer thickness (nm) of the citrus pectin (CP) samples with different degree of methylesterification (DM; 82, 38 or 10%) onto polystyrene (PS) and melamine fluoride (MF) microspheres, measured at both pH 3 as well as pH 7. Different letters in the same column indicate significant differences among the samples (95% confidence interval).

	Adsorbed layer thickness (nm)			
	PS		MF	
	pH 3	pH 7	pH 3	pH 7
CP82	1064.3 ± 84.4 [a]	556.8 ± 26.7 [b]	826.0 ± 141.2 [a]	403.7 ± 52.6 [b]
CP38	989.0 ± 109.2 [a]	868.9 ± 56.7 [a]	865.5 ± 114.6 [a]	828.5 ± 31.9 [a]
CP10	1009.3 ± 134.7 [a]	1045.2 ± 94.4 [a]	885.9 ± 96.4 [a]	1030.5 ± 160.3 [a]

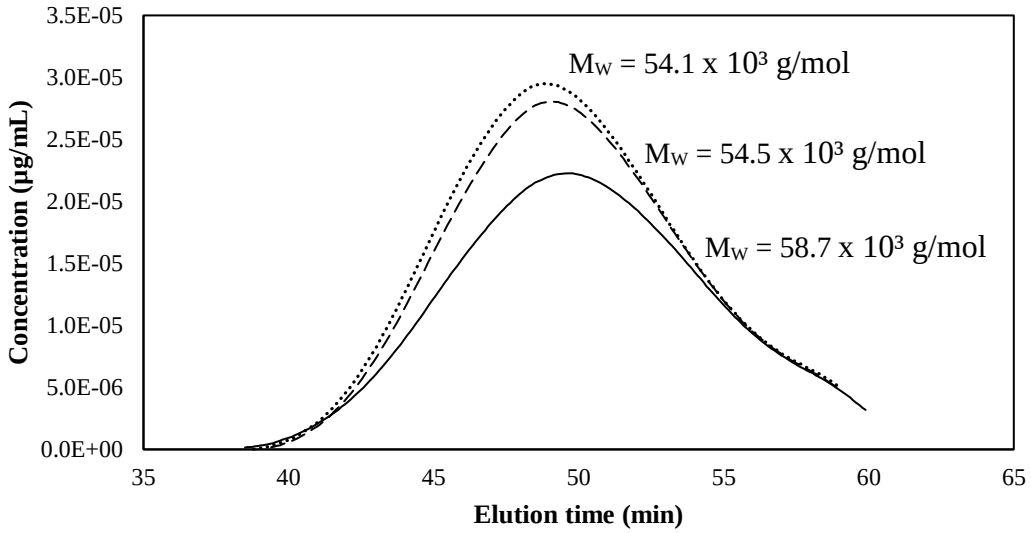

Figure 1: Concentration profile and corresponding weight-average molecular weight (M_w) of the pectin samples (full line: CP82; dashed line: CP38 and dotted line: CP10).

897

898

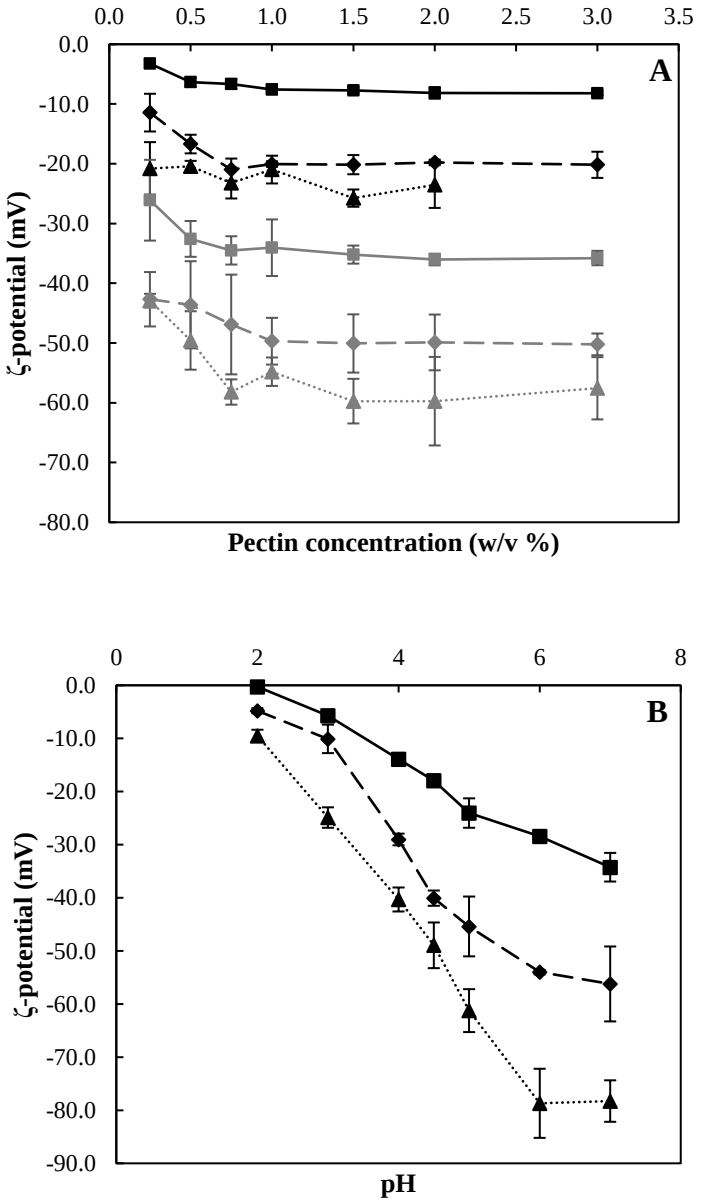

Figure 2: The ζ-potential of different citrus pectin structures with different degree of methylesterification (■ 82%, ◆ 38% or ▲ 10%) as function of (A) pectin concentration (black: pH 3; grey pH 7) and (B) pH of the continuous phase (1% w/v pectin solution).

899

900

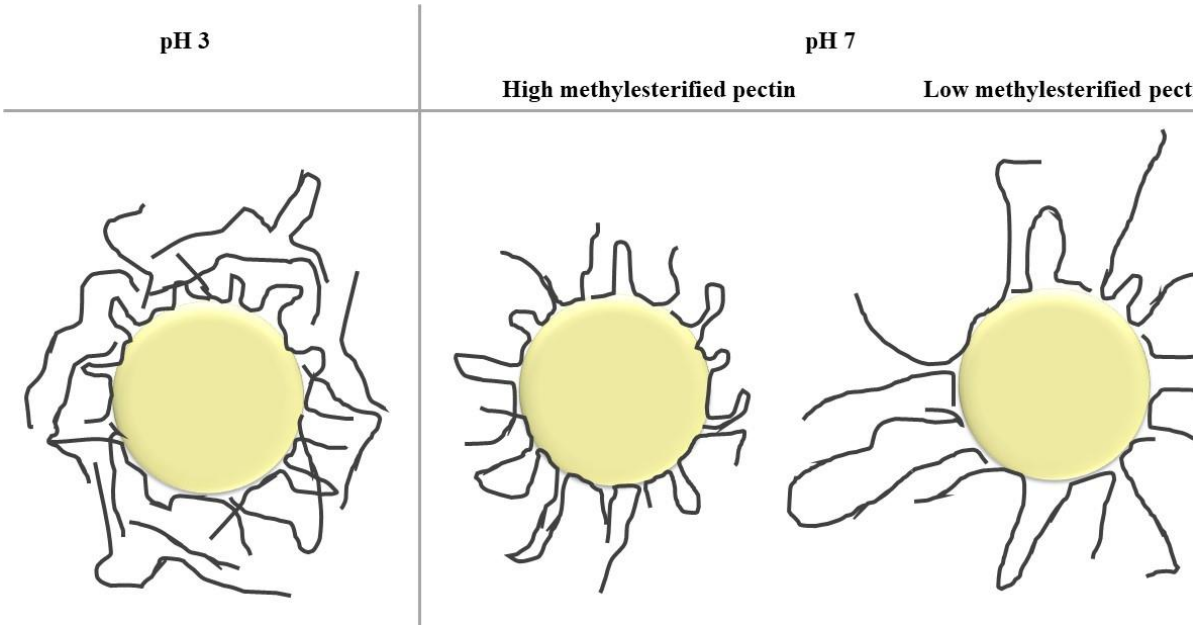

Figure 3: Schematic representation of the hypothetical organization of citrus pectin at the oil-water interface at pH 3 versus pH 7 based on the experimental data obtained in the presented study

901

902

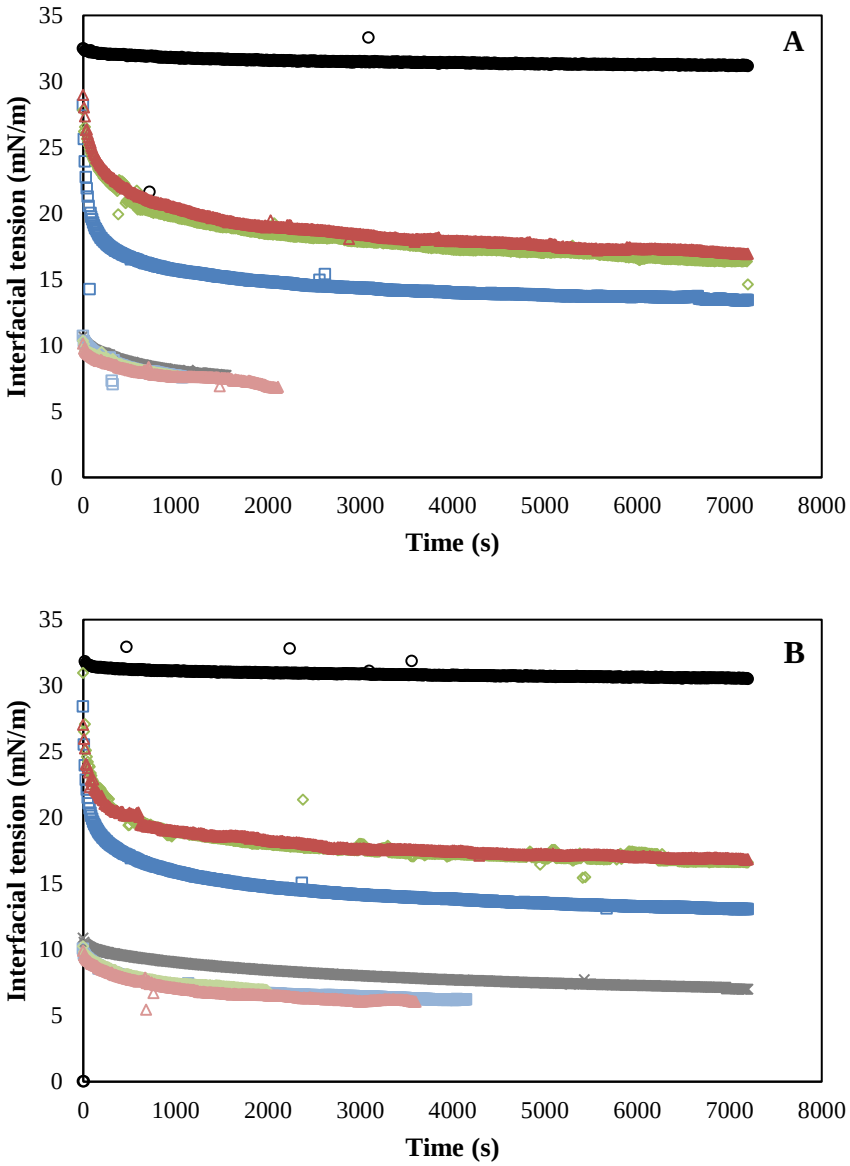

Figure 4: Surface tension as function of time for purified olive oil in presence of water or different emulsifier solutions at (A) pH 3 versus (B) pH 7 (○ MilliQ water; × TW; □ CP82; ◇ CP38; △ CP10; □ TWCP82; ◇ TWCP38 and △ TWCP10). For representation in color is referred to the online version. For interpretation of the abbreviations is referred to the abbreviation list.

903

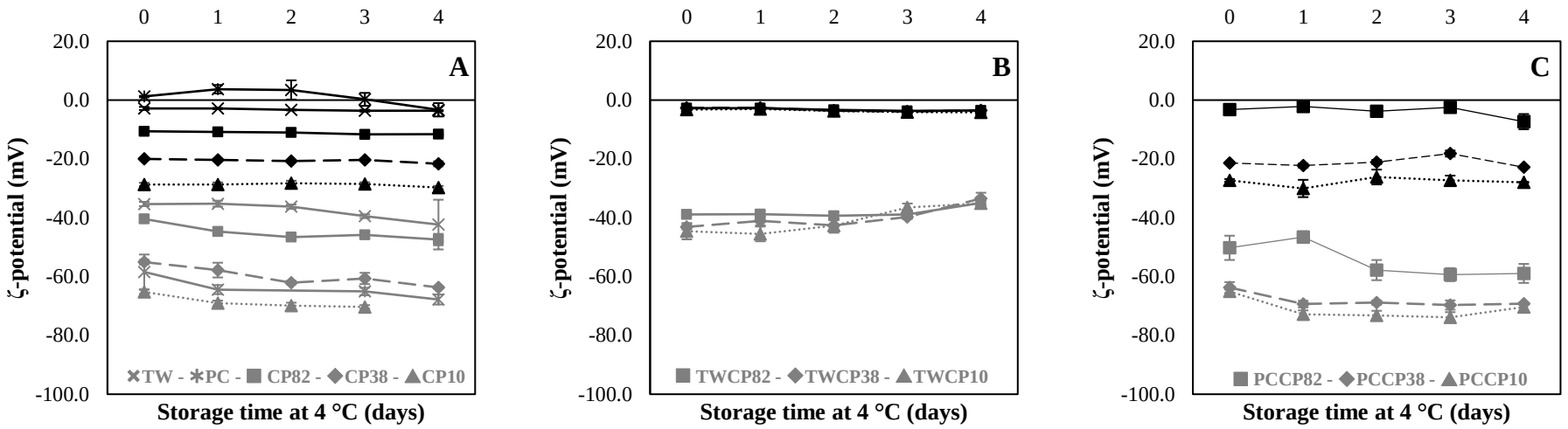

Figure 5: The ζ-potential of the (A) single-emulsifier, (B) Tween-pectin and (C) phosphatidylcholine-pectin stabilized emulsions as function of storage time at 4 °C (black lines represent emulsions at pH 3 and grey lines represent emulsions at pH 7). For interpretation of the abbreviations is referred to the abbreviation list.

904

905

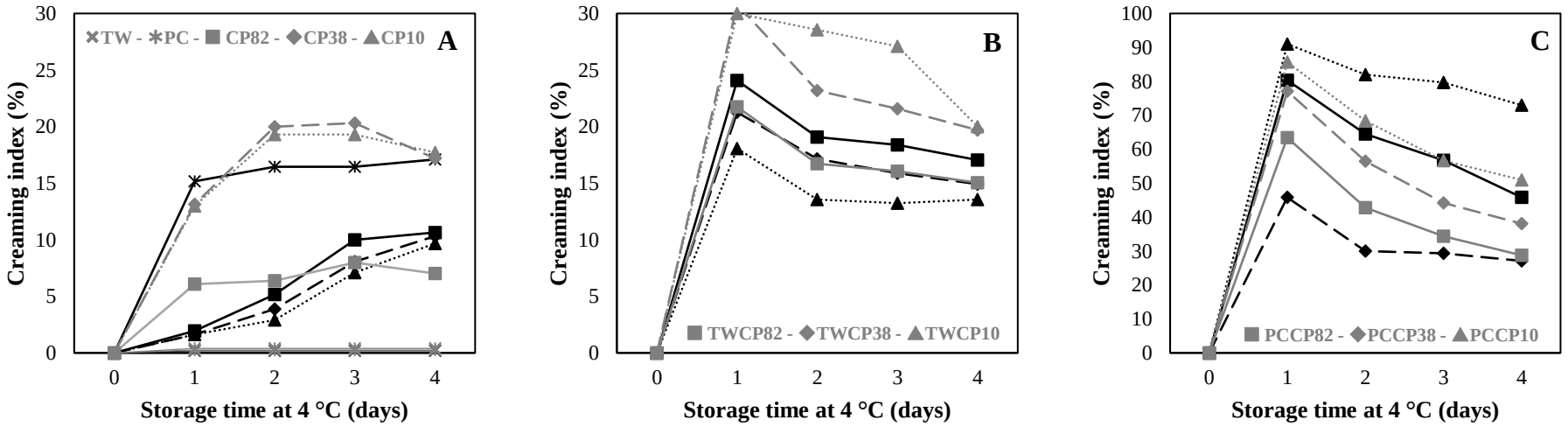

Figure 6: Creaming index of the (A) single-emulsifier, (B) Tween-pectin and (C) phosphatidylcholine-pectin stabilized emulsions as function of storage time at 4 °C (black lines represent emulsions at pH 3 and grey lines represent emulsions at pH 7). For interpretation of the abbreviations is referred to the abbreviation list.

906

907

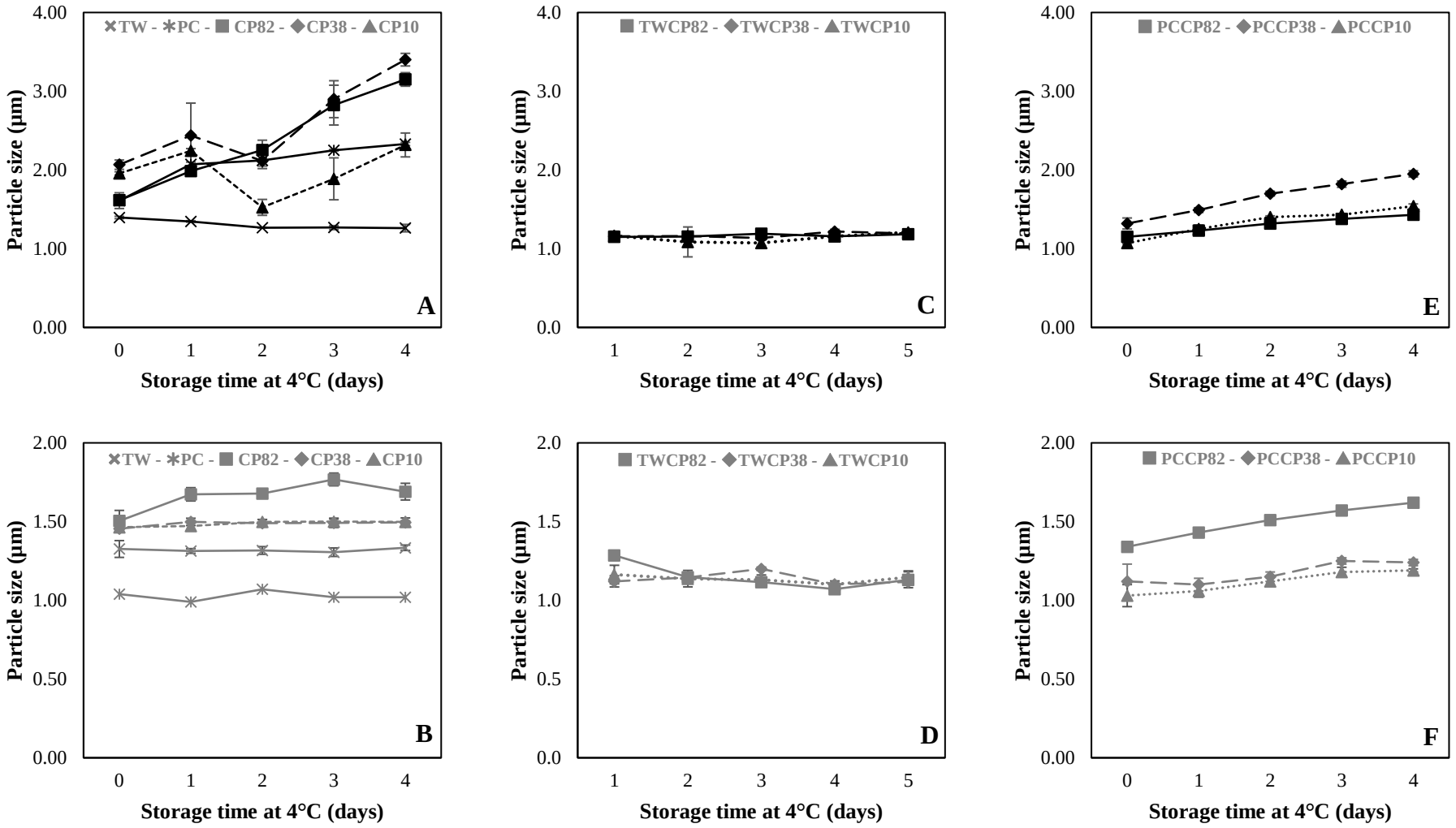

Figure 7: Particle size (d_{43}) of the (A/B) single-emulsifier, (C/D) Tween-pectin and (E/F) phosphatidylcholine-pectin stabilized emulsions as function of storage time at 4 °C (black lines represent emulsions at pH 3 and grey lines represent emulsions at pH 7). For interpretation of the abbreviations is referred to the abbreviation list.

908

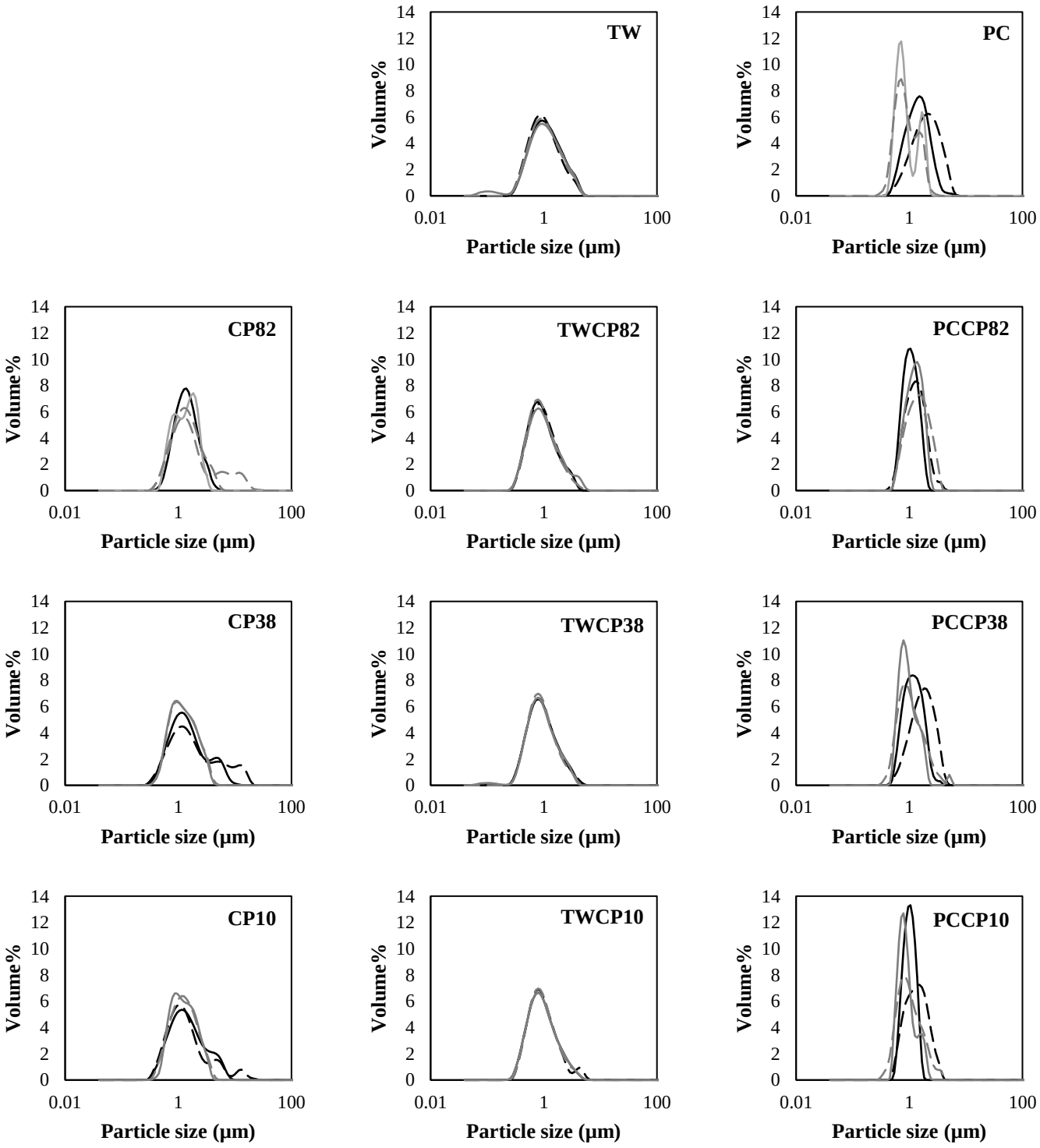

Figure 8: Particle size distribution of each emulsion at the day of preparation (full line) and after 4 days of storage at 4 °C (dashed line) (black lines represent emulsions at pH 3 and grey lines represent emulsions at pH 7). For interpretation of the abbreviations is referred to the abbreviation list.

pH 3										
TW		**PC**		**CP82**		**CP38**		**CP10**		
Day 0	Day 4	Day 0	Day 4	Day 0	Day 4	Day 0	Day 4	Day 0	Day 4	
										
				TWCP82		**TWCP38**		**TWCP10**		
				Day 0	Day 4	Day 0	Day 4	Day 0	Day 4	
										
				PCCP82		**PCCP38**		**PCCP10**		
				Day 0	Day 4	Day 0	Day 4	Day 0	Day 4	
										

pH 7										
TW		**PC**		**CP82**		**CP38**		**CP10**		
Day 0	Day 4	Day 0	Day 4	Day 0	Day 4	Day 0	Day 4	Day 0	Day 4	
										
				TWCP82		**TWCP38**		**TWCP10**		
				Day 0	Day 4	Day 0	Day 4	Day 0	Day 4	
										
				PCCP82		**PCCP38**		**PCCP10**		
				Day 0	Day 4	Day 0	Day 0	Day 4	Day 0	
										

911

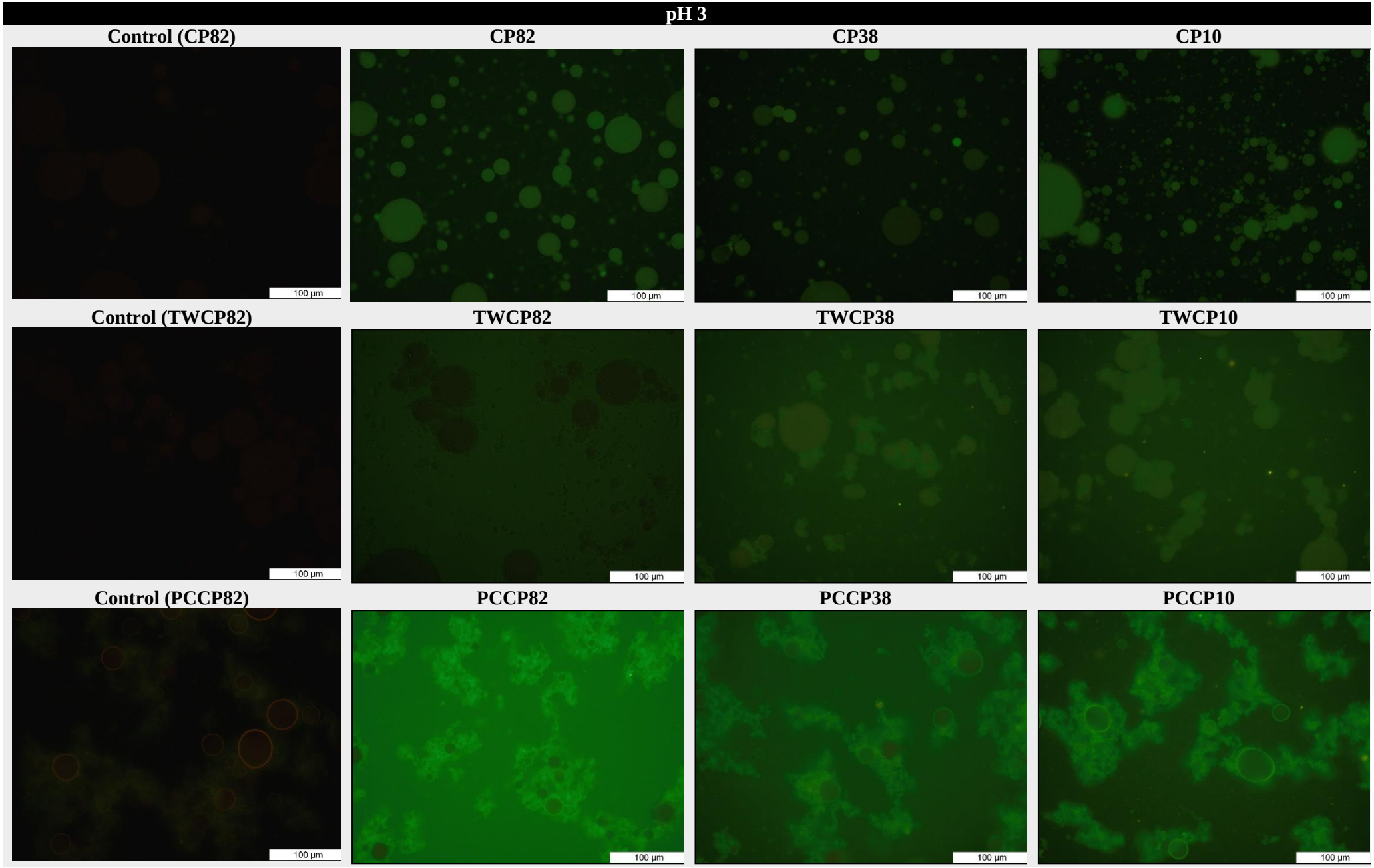
pH 3
Control (CP82)
CP82
CP38
CP10
Control (TWCP82)
TWCP82
TWCP38
TWCP10
Control (PCCP82)
PCCP82
PCCP38
PCCP10
100 µm

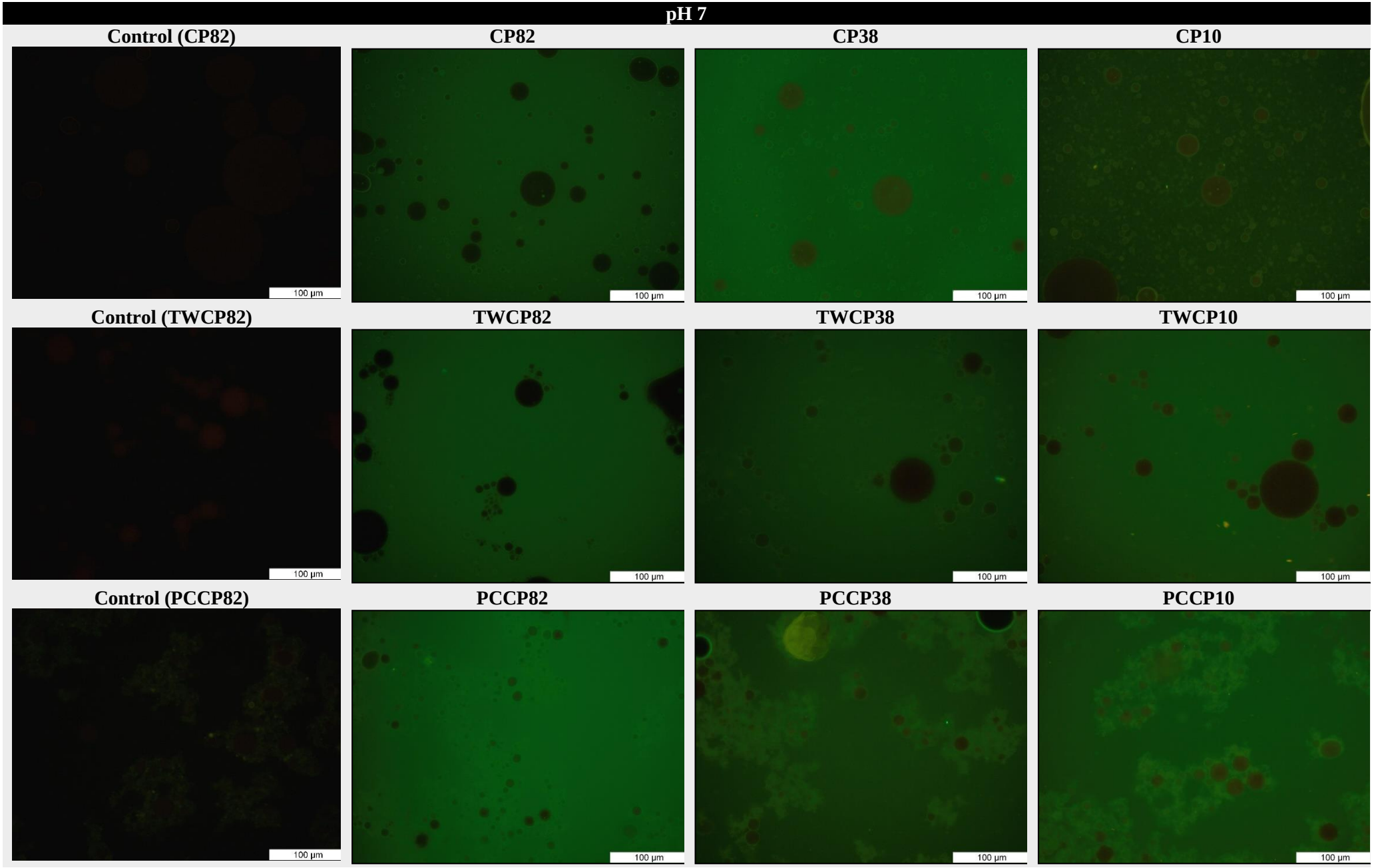
pH 7
Control (CP82)
CP82
CP38
CP10
Control (TWCP82)
TWCP82
TWCP38
TWCP10
Control (PCCP82)
PCCP82
PCCP38
PCCP10
100 µm

912